



Cite this: *Mater. Adv.*, 2022, **3**, 5248

Received 17th March 2022,  
Accepted 13th May 2022

DOI: 10.1039/d2ma00311b

rsc.li/materials-advances

# Chemical labeling and crosslinking of tobacco mosaic virus *via* multi-diazonium reagents: examples, applications, and prospects

Xinyan Qiu,<sup>†</sup> Xueying Kang,<sup>†</sup> Jiqin Zhu\* and Long Yi \*

Tobacco mosaic virus (TMV) is a rod-shaped hollow plant viral nanoparticle (300 nm × 18 nm) and exhibits abundant amino acid residues on the surface of capsid proteins for facile chemical labeling. The use of TMV as a nano-template to produce materials with multiple functions has received particular attention in the past decade. In addition, TMV can be largely produced in gram-scale quantities and is also considered much safe for mammals. Hence, using TMV as building blocks to assemble biomaterials (e.g., hydrogels) has emerged as an attractive field for biomedical applications. This minireview details up-to-date research on the development of bench-stable diazonium reagents and their applications for TMV labeling and crosslinking. The strategy for the preparation of virus-based hydrogels is highlighted. We hope that this review will inspire the development of a large number of plant virus-based biomaterials for various applications in the near future.

## 1. Introduction

Hydrogels are three-dimensional (3D) networks of hydrophilic polymers joined together by covalent bonds or physical intermolecular attraction.<sup>1–5</sup> The presence of hydrophilic moieties such as amide, carboxyl, amino, and hydroxyl groups scattered along the backbone of the 3D networks contributes to the high hydrophilicity of hydrogels.<sup>2</sup> Many hydrogels have good biocompatibility,<sup>3–5</sup> and therefore the biomedical applications of hydrogels have expanded to many fields, including drug delivery,<sup>3</sup> biosensors,<sup>6</sup> wound healing,<sup>7</sup> tissue engineering,<sup>5,8</sup> cell culture,<sup>9</sup> antibacterial materials,<sup>10</sup> and others.<sup>11</sup> These hydrogel materials can be prepared from different building blocks (e.g., cellulose nanofibrils and peptides)<sup>12–14</sup> and using different strategies (Fig. 1).<sup>15–18</sup> For example, enzyme-triggered peptides can form hydrogels through intermolecular weak interactions and self-assembly (Fig. 1a).<sup>19,20</sup> A sort of chain-growth polymerization helps make nanocomposite hydrogels (Fig. 1b).<sup>21</sup> The crosslinking (non-covalent interactions & covalent bond formation) between bifunctional molecules and crosslinkers represents one of the most widely used hydrogel production techniques (Fig. 1c).<sup>4,17,22</sup> In addition, new multiple crosslinking network hydrogels that can overcome the bottlenecks of mechanical performance of single network hydrogels

have flourished in recent years.<sup>23</sup> Moreover, we discovered that the direct chemical crosslinking of plant viruses can be used as

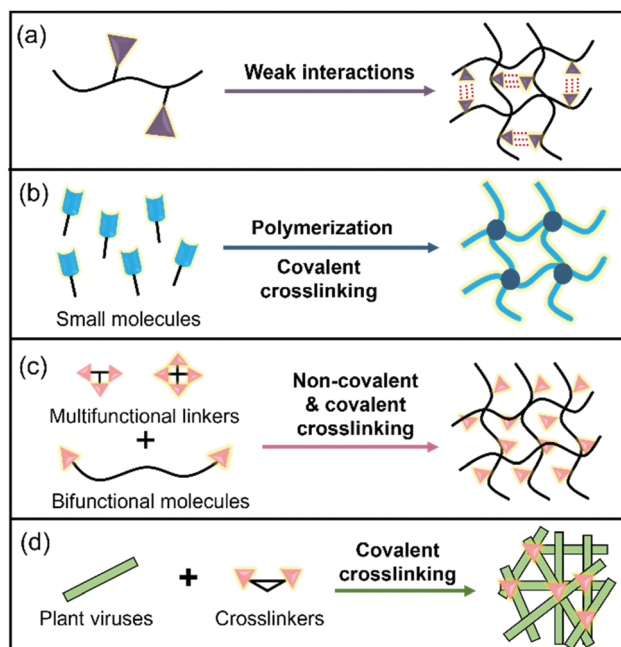


Fig. 1 Construction of hydrogels via different strategies: (a) self-assembly of building blocks via weak interactions; (b) polymerization of small molecules via covalent crosslinking; (c) covalent or non-covalent crosslinking between multifunctional linkers and bifunctional molecules; (d) covalent crosslinking of plant viruses.

State Key Laboratory of Organic-Inorganic Composites and Beijing Key Lab of Bioprocess, Beijing University of Chemical Technology, Beijing 100029, China.  
E-mail: zhujiq@mail.buct.edu.cn, yilong@mail.buct.edu.cn

<sup>†</sup> These authors contributed equally to this work.

a new strategy to prepare hydrogels (Fig. 1d).<sup>24</sup> In the present minireview, we focus on providing a brief summary of the development of bench-stable diazonium reagents and their labeling of tobacco mosaic virus (TMV) for generation of biomaterials including hydrogels.

Plant viruses can be easily obtained in grams with high uniformity and are biocompatible with mammals, and therefore, they have numerous advantages for biological and materials science applications.<sup>25–28</sup> Plant viruses can be divided into zero-dimensional (0D) icosahedral capsids and one-dimensional (1D) rod/filamentous-shaped capsids, both of which are virus nanoparticles (VNPs) that can be tens to hundreds of nanometers in size.<sup>25</sup> Plant viruses are made up of many copies of one or more identical coat protein components that self-assemble into a capsid that encloses the virus genome. Therefore, both genetic engineering and bioconjugation technologies have allowed plant viruses to be amenable to manipulations (Fig. 2), providing virus-like nanoparticles (VLPs) for the advancement of an array of nanotechnology applications.<sup>29–33</sup> In addition, the self-assemblies of viral capsids and viruses have potentially useful characteristics for a variety of nanotechnology applications including encapsulation.<sup>34–36</sup> These plant VNPs and VLPs have also been employed as nanotemplates for biomineralization.<sup>37,38</sup>

TMV is a well-studied plant virus in the past century and was the first viral structure to be examined.<sup>39,40</sup> TMV is composed of 2130 identical coat proteins with a molecular weight of 17 534 Da, which is arranged helically around a single-strand, positive-sense RNA molecule to generate a rod-shaped hollow nanoparticle with 300 nm in length and 18 nm in diameter (Fig. 3). Due to its special 1D structure, good biocompatibility, easily chemical and genetic modifications,

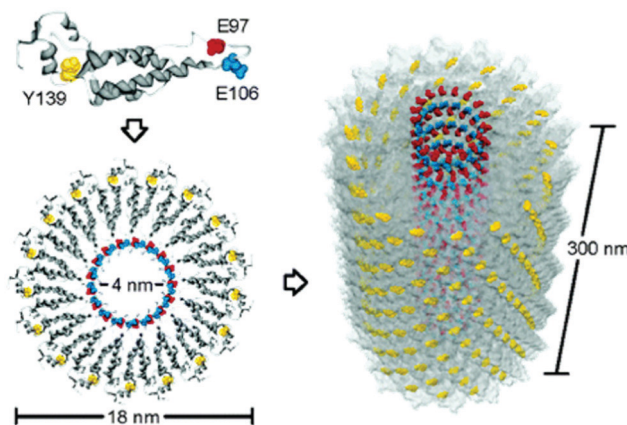


Fig. 3 Schematic illustration of the TMV structures and the potential reactive positions of tyrosine 139 (yellow), glutamate 97 (red), and glutamate 106 (blue) in a capsid monomer.<sup>44</sup> Reprinted with permission from ref. 44. Copyright (2005), American Chemical Society.

TMV has aroused great research interest in self-assembly and as a building block for the construction of bio-nano composite materials.<sup>41</sup> For example, wide-type TMV can be applied as a nanomaterial template for the construction of 1D nanowires and nanotubes.<sup>42,43</sup> In addition, TMV particles contain tyrosine residues (Tyr139) on the external surface and glutamic acid residues (Glu97 and Glu106) at the internal surface (Fig. 3), providing two types of reactive handles for dual modifications on both surfaces.<sup>44,45</sup> For example, a common strategy of Tyr modification is by using *in situ* diazonium generation and coupling,<sup>46,47</sup> which may affect the structure of the protein as well as make it difficult to control the stoichiometry of the reaction. To solve this problem, several bench-stable diazonium salts have recently been developed for TMV labeling and crosslinking.<sup>24</sup> On the other hand, Cys and Lys residues were genetically engineered onto the virion surface of TMV mutants, producing additional attachment sites for mineralization<sup>48,49</sup> and bioconjugation.<sup>50–53</sup> As a result, TMV and mutants are widely functionalized by small molecules, polymers, peptides, MRI contrast agents, antigens, and therapeutics for various applications.<sup>54–64</sup> We note that there are a series of excellent reviews for TMV-based nanomaterials during the last decade.<sup>60–64</sup> However, the current development of stable diazonium reagents for TMV labeling is not summarized. In addition, the 1D lengths and the diameters of the TMV nanoparticle can be tuned and controlled *via* self-assembly and chemical labeling to generate virus-like particles (VLPs),<sup>65–67</sup> which can break the limitation of fixed sizes of natural virus templates. Moreover, dual-diazonium reagents for TMV crosslinking provide an additional strategy for the preparation of hydrogels.<sup>24</sup> This recent new progress can inspire various new biomaterials for research in different directions but has not been specially reviewed in previous papers.

Here, we will provide a full description of the development of stable diazonium reagents from our group as well as others, which may help readers to clearly understand their properties and potential applications in chemical biology and materials

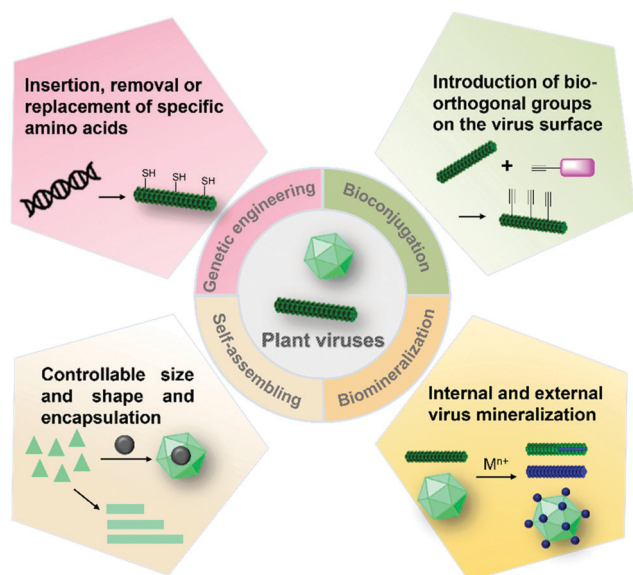


Fig. 2 Modifications and construction of plant VNPs and VLPs. VNPs and VLPs can be generated by genetic engineering, bioconjugation, and self-assembly, all of which can be further functionalized by chemical labeling, biomineralization, or encapsulation.<sup>25</sup>



science. This minireview also summarizes the recent research on chemical modifications of TMV Tyr139, the construction of controllable TMV-based VLPs, and virus-based hydrogels. The synthesis and methods for making these reagents and biomaterials are described in detail. Because bioorthogonal chemical reactions have emerged as excellent tools for biolabeling,<sup>68–75</sup> we discussed the combination between bioorthogonal reactions and diazonium salt reagents. We also outline the future directions for crosslinking of plant viruses *via* multi-diazonium reagents. We anticipate that this minireview will promote the further development of plant virus-based biomaterials for a variety of applications.

## 2. Development of diazonium salts and reagents for TMV modifications

A traditional diazonium coupling reaction to tyrosine residues of TMV is very useful for the construction of new materials.<sup>44,45</sup> For example, Francis and coworkers reported that efficient modifications of TMV capsids were accomplished through a mixture of intact viral capsids and 35 equiv. of diazonium salts (*in situ* synthesis at 0 °C) in pH 9 buffer for 2 h.<sup>44</sup> The formation of **2** using **1** provides ketone sites for further convenient conjugation *via* the oxime ligation (Fig. 4a). For example, upon exposure of **2** to polyethyleneglycol (PEG)- or biotin-containing alkoxyamines, adducts **3** and **4** were obtained with virtually complete conversion, and >2000 copies of biotin were installed on the capsid exterior. In addition, the generated PEG-labeled capsids **3** was organically soluble TMV rods that may greatly expand the conditions for further bioconjugation reactions as well as future device fabrication in the organic phase.

Cu<sup>I</sup>-catalyzed azide-alkyne 1,3-dipolar cycloaddition (CuAAC), namely the click reaction, has been widely used for highly efficient bioconjugation.<sup>76</sup> To this end, Wang and

coworkers reported that TMV was first treated with diazonium salt **6** (*in situ* generated from **5**) to obtain alkyne-labeled capsids **7**, and then the tandem CuAAC reactions were employed for TMV modifications to obtain single and double click adducts **8** and **9** (Fig. 4b).<sup>77</sup> This optimized method was successfully used to program the surface properties of TMV that can modulate cell behaviors grown on TMV-based biomaterials. Further examples of diazonium labeling include the installation of antigens<sup>78</sup> and peptides<sup>79</sup> on the TMV Tyr residues. Moreover, free radical oxidation of the TMV Tyr also led to acrylate-functionalized viruses with customizable properties.<sup>80</sup>

Though the TMV modifications using diazonium coupling are successful,<sup>77–79</sup> one barrier to the widespread use of these diazonium salts is the prerequisite of *in situ* preparation from anilines under strongly acidic conditions at 0 °C before use. In addition, such *in situ* synthesized salts may bring difficulty in controlling the stoichiometry of the reaction. To this end, Barbas and coworkers developed the first bench-stable crystalline diazonium salt (**11**) that can be used for tyrosine-selective modification of peptides and proteins to introduce the aldehyde tags suitable for classical oxime and hydrazone ligations.<sup>81</sup> **11** was synthesized on a gram scale from commercially available 4-aminobenzaldehyde polymer **10** (Fig. 5a), and the hexafluorophosphate counterion was essential for the stability of the diazonium salt. Direct mixture of **11** and proteins generated the labeled protein **12** with the aldehyde tags suitable for the classical hydrazone ligation to obtain **13** (Fig. 5b). Compared with the diazonium coupling using the *in situ* synthesized salts, the protein labeling by the reagent **11** is much more facile for experimental operation. In addition, this bioconjugate technique was used for the facile introduction of functional tags onto model proteins and even to label the surface of live cells.

Consequently, Xi, Yi, and coworkers reported that a bench-stable diazonium reagent **14** could be used to label the TMV

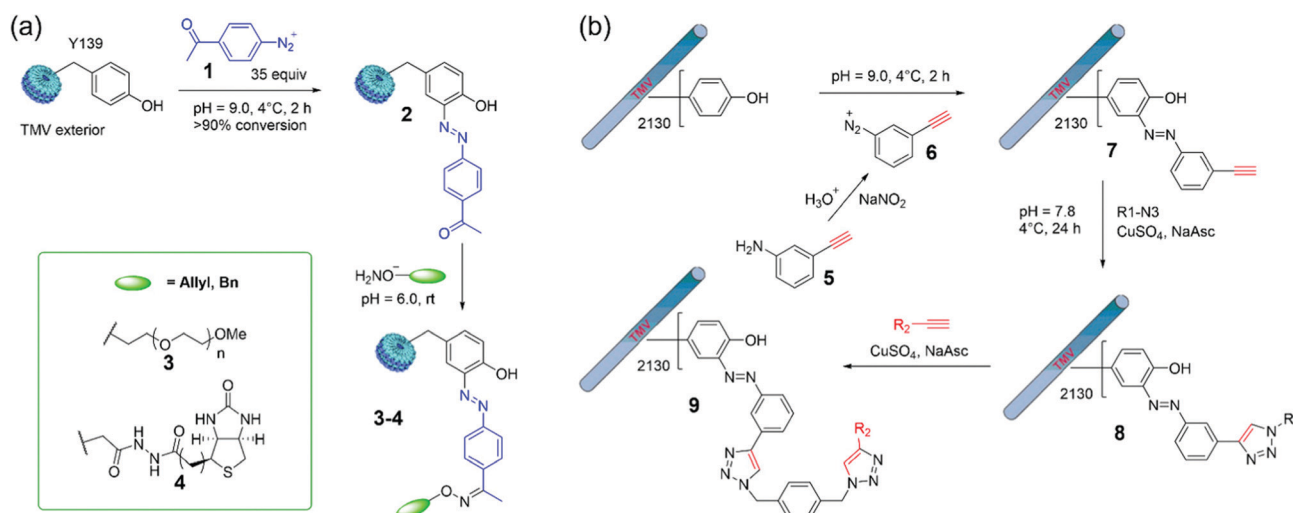


Fig. 4 (a) Site-selective azo-coupling on Y139 in the TMV exterior with *in situ* generated diazonium salts **1** and further labeling *via* oxime ligation.<sup>44</sup> (b) Formation of a diazonium salt **6** *in situ* and the bioconjugation of TMV by means of CuAAC reactions.<sup>77</sup> Reprinted with permission from ref. 77. Copyright (2008) Wiley-VCH Verlag GmbH & Co. KGaA, Weinheim.





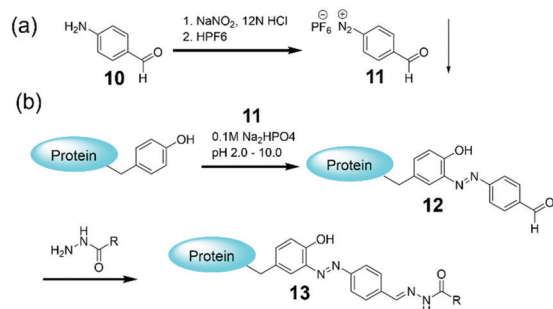


Fig. 5 (a) Synthesis of a diazonium reagent **11**. (b) Protein labeling via the reagent **11** followed by an efficient hydrazone ligation chemistry.<sup>81</sup>

surface to incorporate thiols for further fluorescence labeling by **15** and gold coating (Fig. 6a).<sup>65</sup> On the other hand, based on insights into the TMV assembly mechanism,<sup>40</sup> we envisioned that the length of the TMV particle can be controlled by the length of the encapsulated viral RNA, and the Xi group at Nankai University has made efforts to use *in vitro* transcribed RNAs at different but controllable lengths to achieve VLPs with controllable lengths (Fig. 6b).<sup>82</sup> It is noted that Yi and coworkers had also synthesized controllable short TMV-like nanorods (less than 60 nm) based on the self-assembly,<sup>67</sup> but we prepared virus-like assemblies up to 400 nm (longer than the wide-type TMV) in a controllable fashion. Furthermore, we can easily modulate both the length of VLPs and the type of surface functionality *via* the reagent **14**. For example, thiol-labeled VLPs were incubated with Cd<sup>2+</sup> followed by treatment

with H<sub>2</sub>S to generate a thin layer of CdS coating on the surface of VLPs. It is noted that CdS could be coated on different lengths of virus-like assemblies to generate CdS nanorods with controllable sizes, which represents a new synthetic route for a material tenability. Additionally, there should be plenty of room in the field of the combination of VLPs and chemical labeling for the controllable synthesis of nanocomposites.

Direct introduction of the click groups into proteins/viruses is the key step for further facile bioconjugation. For addressing this issue, Yi, Xi, and coworkers have reported a diazonium salt reagent for facile covalent incorporation of alkyne groups into proteins under mild conditions.<sup>83</sup> The reagent **17** was facilely synthesized from commercially available and cheap **16**, yielding light-yellow precipitates (57% yield) with good stability under common conditions (Fig. 7a). The small-molecule model studies allowed us to determine the reaction rate as 5.7 M<sup>-1</sup> s<sup>-1</sup> at pH 8.0, which is about 4.7-fold faster than that at pH 7.0. Moreover, strong fluorescence labeling of bovine serum albumin (BSA) was achieved after the reaction with **17** followed by the click reaction with **20** in one pot (Fig. 7b). More importantly, fluorescence labeling of TMV coated proteins was also achieved by the method (Fig. 7c), and transmission electron microscopy image (TEM) showed that TMV particles were not destroyed by the labeling reactions (Fig. 7d). Considering the mild reaction conditions and facile operations of the labeling strategy, we expect that the method based on the reagent **17** can be extended to other protein materials and plant viruses in the future.

Though several bench-stable diazonium reagents were successfully applied to directly incorporate aldehyde, ketone, or alkyne groups into Tyr residues of proteins, the next-step bioorthogonal reactions based on these reagents may suffer from low reaction efficiency or the need for catalysis. The inverse electron demand Diels-Alder reaction (IEDDA) or tetrazine-ene reaction is one of the best bioorthogonal reactions for catalyst-free covalent ligation.<sup>72,74,84,85</sup> Therefore, Yi, Lv, and coworkers developed a tetrazine-containing diazonium reagent **21** (Fig. 8a).<sup>86</sup> The bench-stable and water-soluble **21** was successfully employed for the direct, efficient and covalent introduction of tetrazines onto target proteins or virus surfaces. This tetrazinylation was further applied for the tetrazine-ene ligation to achieve protein PEGylation under very mild conditions. The tetrazine-containing TMV was confirmed using mass spectra with an increased mass of 420 Da of the TMV coat protein (the calculated mass, 417 Da) as well as fluorescence labeling using the norbornylene-containing fluorescent dye. In addition, we further demonstrated the utility of **21** through its direct incorporation into total cell lysates. Compared with **17**, reagent **21** is more advantageous because the tetrazine-ene ligation is catalyst-free and has tunable rates by choosing different alkenes or alkynes in need. We believe that Tyr labeling based on **21** could provide a useful toolbox for the preparation of new materials in the future.

Though the tetrazine-ene ligation is useful for labeling of TMV, other catalysis-free, efficient, and facile bioorthogonal reactions may also be applied for such bioconjugation. In 2017,

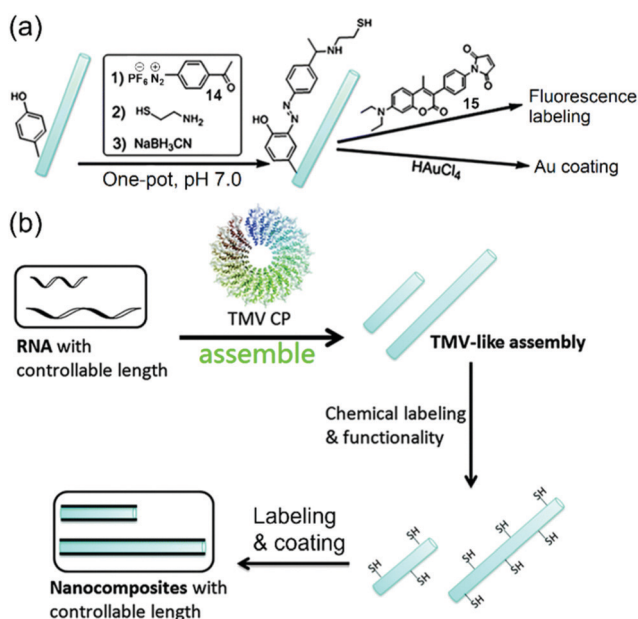
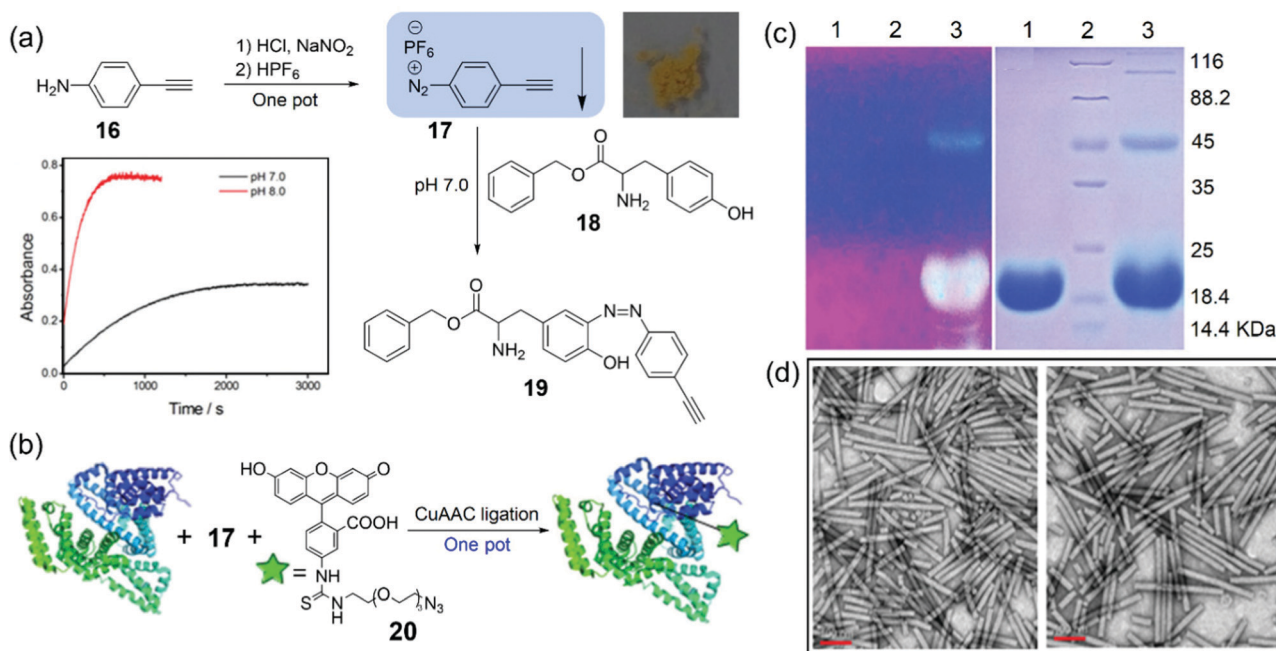


Fig. 6 (a) The schematic drawing of the TMV labeling via the reagent **14** followed by cysteamine and reduction in one pot to produce thiolated TMV (TMV-SH). The TMV-SH could react with 7-diethylamino-3-(4-maleimidophenyl)-4-methylcoumarin (**15**) or chloroauric acid (HAuCl<sub>4</sub>). (b) A strategy for the fabrication of size-controllable 1D nanocomposites based on TMV-like assemblies as templates.<sup>65</sup> Reprinted with permission from ref. 65. Copyright (2014), Royal Society of Chemistry.



**Fig. 7** (a) Synthesis of a diazonium reagent **17** and its reaction with Tyr-containing **18** to generate **19**, as identified using the HRMS spectrum. Inset: The intensities at 400 nm versus reaction time for **17** upon treatment with **18** in PBS at pH 7.0 (black line) or pH 8.0 (red line). (b) The fluorescence labeling reactions of BSA via **17** followed by **20** in one pot. (c) 10% SDS PAGE of TMV before (lane 1) and after (lane 3) fluorescence labeling by **17** and **18** under a UV lamp or Coomassie blue staining, respectively. (d) TEM images of TMV before and after fluorescence labeling, respectively.<sup>83</sup> Reprinted with permission from ref. 83. Copyright (2014), Royal Society of Chemistry.

Yi, Wang, and coworkers found that the *o,o'*-difluorinated aryl azide could react efficiently with triphenylphosphine to produce a water-stable phosphanimine, which is called nonhydrolysis Staudinger reactions (NSRs).<sup>87</sup> Consequently, Xi, Yi, and coworkers employed a tetrafluorinated aryl azide for the development of a faster NSR for protein and RNA labeling.<sup>88</sup> The reaction kinetics of this NSR could be monitored by a fluorescence method to generate the reaction rate as  $51.8 \text{ M}^{-1} \text{ s}^{-1}$ , which is the fastest Staudinger ligation in aqueous buffer up to date. It is noted that Yan, Ramström, and co-workers independently discovered a similar NSR and determined the reaction rate as  $18 \text{ M}^{-1} \text{ s}^{-1}$  by an NMR method.<sup>89</sup> All the above NSR are facile, fast, and bioorthogonal for bioconjugation *in vitro* and in live cells.

To extend the applications of the NSR, Yi, Zhu, and coworkers envisioned that the *o,o',m,m'*-tetrafluorinated aromatic azides could be incorporated into proteins and viruses through the diazonium coupling for subsequent NSR labeling. To this end, we developed a highly efficient and bench-stable reagent **22** and investigated the small-molecule model reaction between **22** and Tyr-containing **18** to generate **23** (Fig. 8b).<sup>90</sup> Consequently, protein fluorescence labeling, PEGylation, and biotinylation were achieved by further functionalization of the azido-labeled proteins *via* the fast NSR by **24–27** (Fig. 8c). To our delight, the whole protein labeling processes could be finished in one pot within several hours under catalysis-free conditions.

Though TMV nanoparticles have been widely used as templates for controllable syntheses of nanomaterials,<sup>60–65</sup> the

diameters of native viruses are restricted to 18 nm. To address this issue, the highly efficient method based on **22** was applied to adjust the size of native viruses (Fig. 8b). The Tyr139 residues of TMV were labeled by **22** followed by **27** (Fig. 8c), and TEM analysis suggested that the diameter of **22–27**-TMV rods was increased to  $21.8 \pm 3.5 \text{ nm}$ . Such thickening of viral particles can provide new nano-templates with tunable sizes and shapes compared with that of the wide-type virus.<sup>65,90</sup> Compared with that based on reagent **21**, the labeling strategy based on the diazo-azide reagent **22** is more facile for the synthesis procedures of the reagents. On the other hand, the reagent **21** provides hydrophilic handles on proteins while the reagent **22** provides hydrophobic handles on proteins. Therefore, the reagent **22** would also expand the toolbox for protein bioconjugation in chemical biology and biomaterials under different conditions.

### 3. Preparation of hydrogels from TMV and dual-diazonium reagents

Based on the success of the development of several bench-stable diazonium reagents for TMV modifications, we envisioned that dual-diazonium and multi-diazonium reagents might be developed for protein and virus crosslinking.<sup>24,91</sup> In 2018, Xi, Yi, and coworkers reported a new water-soluble reagent **28** with double diazonium sites (Fig. 9a) that might link two Tyr residues to lead to the crosslinking of TMV particles **29** (Fig. 9b).<sup>24</sup> The solid **28** was stable for bench use



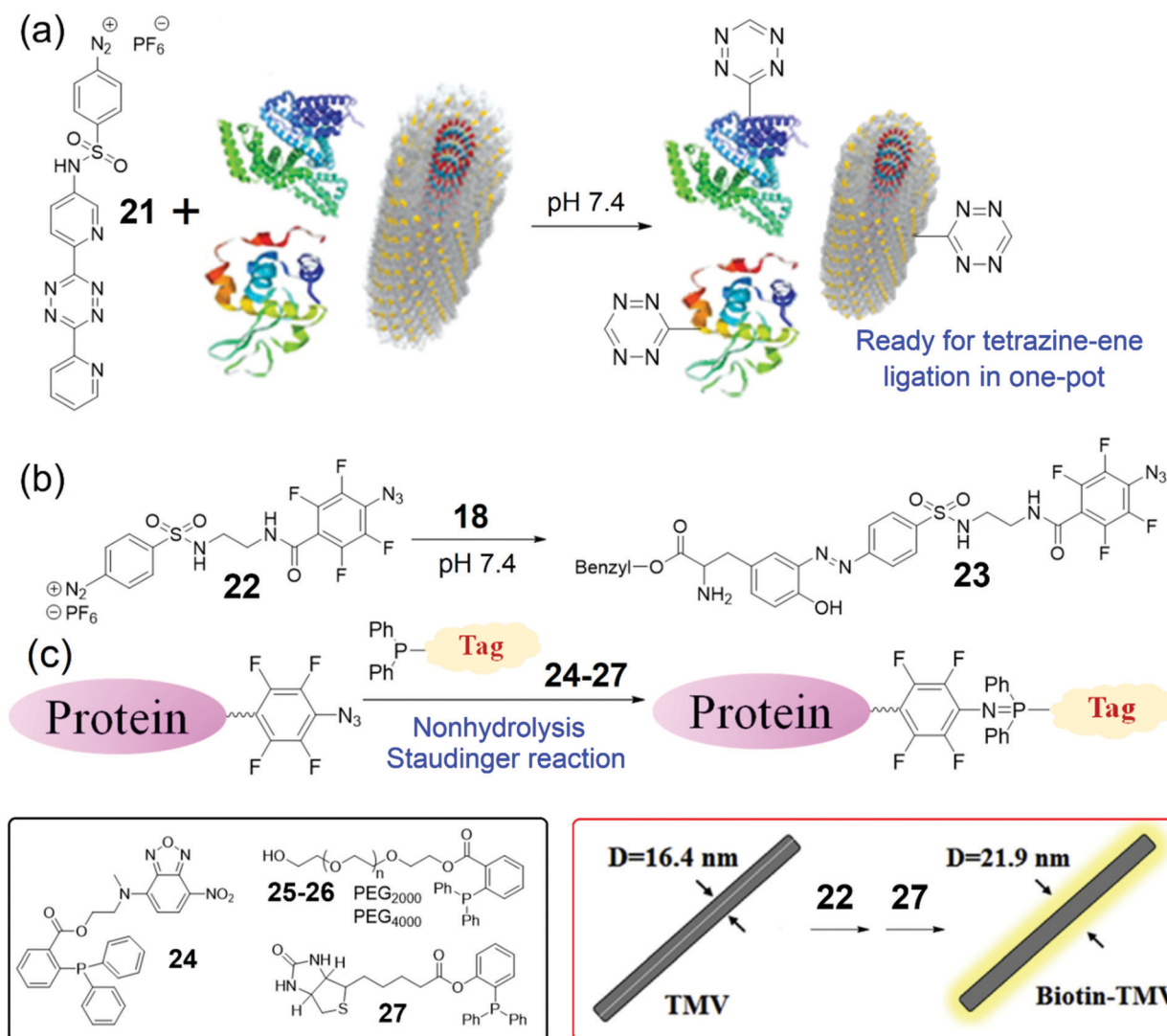


Fig. 8 (a) A tetrazine-containing diazonium reagent **21** for protein/Tyr labeling.<sup>86</sup> (b) Reaction of an azide-containing reagent **22** and **18** to form the azo product **23**. (c) Schematic illustration of the NSR labeling of tetrafluorinated aromatic azide-labeled proteins. Chemical structures of reagents **24-27** and the biotinylation of TMV are also shown.<sup>90</sup>

and storage at  $-20\text{ }^{\circ}\text{C}$  for more than three months. The reactivity of **28** with Tyr is efficient with a rate of up to  $19.6\text{ M}^{-1}\text{ s}^{-1}$ . We proposed that a 3D network could be formed based on the efficient crosslinking of **28** and TMV (Fig. 9c). We optimized the gelation conditions and found that a direct mixture of the reagent **28** (2.5 mM) and TMV (2.5 mg mL $^{-1}$ ) at  $37\text{ }^{\circ}\text{C}$  in neutral buffer (pH 7.0) for 30 min incubation led to the formation of a hydrogel (Fig. 9d).<sup>24</sup> The TMV-based hydrogel was characterized by protein crosslinking and TEM images of 3D networks. In addition, scanning electron microscopy (SEM) analysis further supported the formation of 3D networks of the hydrogel.

For the first virus-based hydrogel, we found that the **28-TMV** hydrogel formation depended on both the crosslinking agent and the highly organized nanostructure of virus particles, and cleavage of the azo bonds by  $\text{Na}_2\text{S}_2\text{O}_4$  was useful for gel degradation. The hydrophobic anticancer drug camptothecin

(CPT)<sup>92</sup> did not affect the gelation and could be packaged using the **28-TMV** hydrogel system, which implied the existence of enough hydrophobic cavities in the hydrogel. More importantly, for the CPT-containing **28-TMV** hydrogel, half of the CPT release could be detected after 12 hours of dialysis, and 72% of the CPT release could be achieved after 3 days of dialysis. Moreover, the TMV-based hydrogel was safe for tobacco plants because TMV crosslinking could completely inactivate virus infection toward plants. Because the crosslinker reagent **28** can be easily prepared from commercial chemicals and is stable, we believe that this strategy of direct crosslinking of viruses and **28** may provide a general approach to prepare various kinds of hydrogels for the future biomedical and agriculture applications.

Though the TMV-based hydrogel can be formed by using **28**, we envisioned that more reactive linkers would result in more efficient gelation of TMV. To this end, Xi, Yi, and coworkers



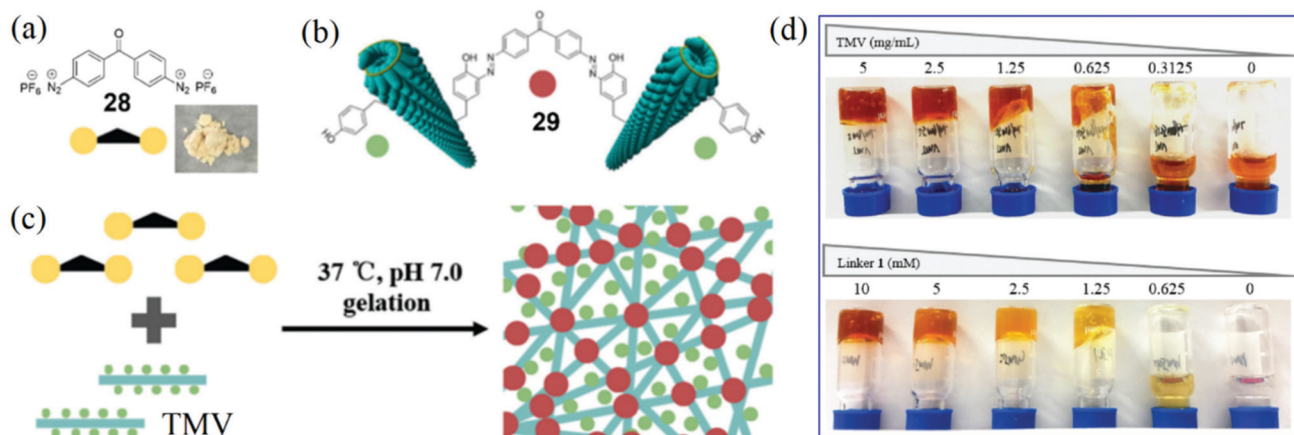


**Fig. 9** (a) Chemical structure of a dual-diazonium crosslinker **28** and photograph of the solid reagent. (b) Illustration of the crosslinking of two virus particles via the crosslinker. (c) Schematic representation of hydrogel formation from the reaction of **28** and TMV.<sup>24</sup> (d) Photographs illustrating the effects of concentrations of TMV and **28** on the gelation. Reprinted with permission from ref. 24. Copyright (2018), Royal Society of Chemistry.

rationally designed and synthesized three new dual-diazonium reagents (**30–32**) to investigate the effects of substituents ( $\text{CO}$ ,  $\text{PO}$ , and  $\text{SO}_2$ ) on the crosslinking efficiency and gelation conditions (Fig. 10a).<sup>91</sup> We found that **30** showed much smaller  $k_2$  ( $18 \text{ M}^{-1} \text{ s}^{-1}$ ) than that of **31** ( $71 \text{ M}^{-1} \text{ s}^{-1}$ ), implying that substituents linked to aromatic cycles could influence the activity of diazonium with Tyr. Compared with **28**,<sup>24</sup> the substitution of the  $\text{CO}$  group with the  $\text{SO}_2$  group greatly enhanced the reaction rate. In addition, the Hammett parameters of the substituents and the reaction rates can be correlated to generate the reaction constant ( $\rho = +0.45$ ),<sup>91</sup> which suggests that the electron-withdrawing substituents can accelerate the crosslinking reaction.

Because of the faster diazonium-tyrosine coupling reaction, hydrogels from the crosslinking of TMV and the reagent **31** could be formed within 1 min at room temperature. We also

tested the rheological characters of the hydrogels formed by TMV and **30** or **31** from the solution phase to gel phase. As shown in Fig. 10b, the TMV-based hydrogel with **31** showed higher viscosity (about 2.5-fold) than that with **30**, and the hydrogel based on **31** had a much faster gelation speed with a relatively higher storage modulus than that based on **30**. SEM images showed that multiple virus rods in the **30**-based hydrogel was crosslinked to form a 3D net structure, while a large number of sheets and less net structure was observed in the **31**-based hydrogel (Fig. 10c). Therefore, the crosslinking reagents could be used for tuning the properties of TMV-based hydrogels. Furthermore, we also developed a crosslinker **32** by introducing a disulfide bond on the basis of **31**. The TMV-based hydrogels prepared from **32** could be used to make the capitals “BUCT” and “NKU” in the dish (Fig. 10d), which could be degraded by reduction of the disulfide bonds using

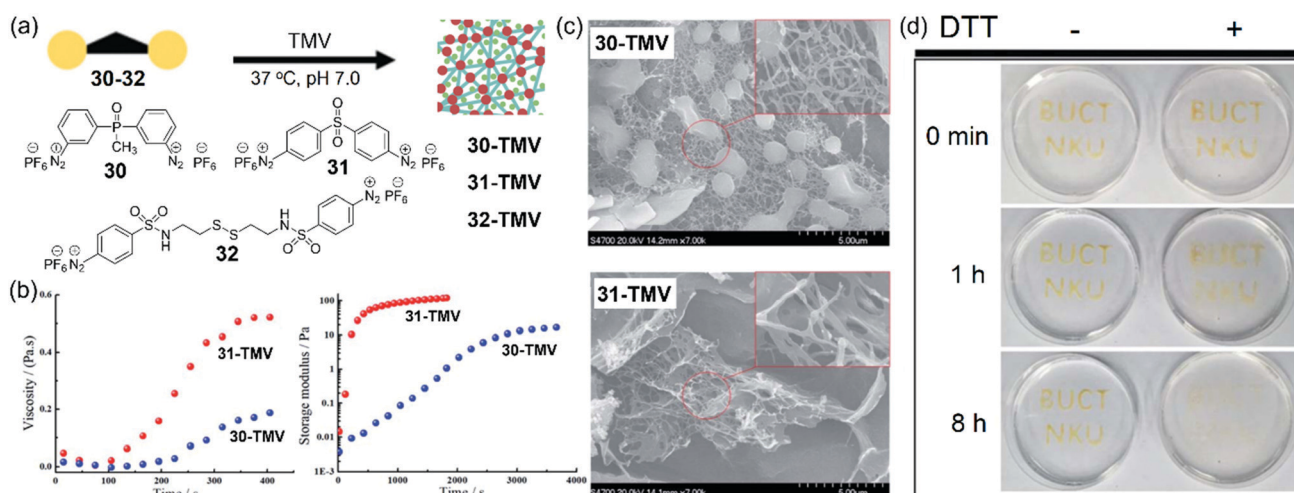


**Fig. 10** (a) Chemical structures of dual-diazonium reagents **30**, **31**, and **32** and their application for the gelation of TMV. (b) Rheological characteristics of two TMV-based hydrogels from **30** and **31**. (c) SEM characterization of the TMV-based hydrogels. (d) Photographs for the TMV-based hydrogel degradation via DTT. The capitals were made from the crosslinking of TMV and **32** on the Petri dish. After gelation, the TMV hydrogel was immersed with DTT solution or deionized water.<sup>91</sup> Reprinted with permission from ref. 91. Copyright (2019), Royal Society of Chemistry.

**Table 1** Summary of properties and applications for synthetic diazonium reagents

Reagent number	Yield (%)	Color (solid)	$k_2$ , (M <sup>-1</sup> s <sup>-1</sup> )	The tandem reactions	TMV functionalization
<b>11</b>	42	Off-white	N.D.	Oxime ligation; hydrazide ligation	N.D.
<b>14</b>	22	Light-grey	N.D.	Imine formation; oxime ligation; hydrazide ligation	Fluorescence labeling; Au coating; CdS coating
<b>17</b>	57	Light-yellow	5.7 (pH 8.0)	CuAAC ligation	Fluorescence labeling; PEGylation
<b>21</b>	46	Red	N.D.	Tetrazine-ene ligation	Fluorescence labeling
<b>22</b>	50	Yellow	N.D.	Nonhydrolysis Staudinger reaction	Fluorescence labeling; PEGylation; biotinylation
<b>28</b>	46	Light-yellow	19.6	—	Virus-based hydrogels
<b>30</b>	60	Off-white	18.4	—	Virus-based hydrogels
<b>31</b>	78	Yellow	71.2	—	Virus-based hydrogels
<b>32</b>	86	Yellow	N.D.	—	Virus-based hydrogels

N.D., no detection.

dithiothreitol (DTT). We also propose that these bench-stable dual-diazonium reagents may provide a general approach to preparing diverse functional hydrogels from other biocompatible viruses for future biomedical applications.

## 4. Summary and outlook

This minireview summarizes the development and applications of stable diazonium reagents for TMV labeling and crosslinking to generate new biomaterials. We as well as others have synthesized a series of bench-stable diazonium reagents from the corresponding anilines in medium to high yields (Table 1). The hexafluorophosphate counterions are important for the stability of solids of these diazonium reagents. Protein labeling by the bench-stable diazonium reagents can be achieved at pH 7.4. The diazonium-tyrosine coupling efficiencies can be tuned by the different substituted moieties on the aryl ring, and the coupling rate was higher with stronger electron-withdrawing substituents. The sulfonyl group at the *p*-position of aryldiazonium salts should be a useful structural motif for highly efficient labeling of protein Tyr residues to incorporate into a functional handle. In addition, these reagents provide a toolbox for the introduction of various bioorthogonal groups into proteins for chemical biology and materials science (Table 1).

Though bioorthogonal groups including aldehydes,<sup>81</sup> ketones,<sup>65</sup> alkynes,<sup>83</sup> tetrazines,<sup>86</sup> and tetrafluorinated aryl azides,<sup>90</sup> have been successfully employed for bench-stable diazonium reagents, we believe that new diazonium reagents using other bioorthogonal groups (Table 2)<sup>93–105</sup> can be further developed for biolabeling under different conditions. Based on our experiences, there should be at least two-point criteria for the bioorthogonal groups in diazonium reagents: (1) the groups should be acid resistant because of the strong acid synthesis conditions of diazonium salts; (2) the groups should not react with diazonium. In future work, functional groups like aryl iodide and aryl boronic acid can be used to synthesize new diazonium for biolabeling *via* bioorthogonal organopalladium reactions (*e.g.* Mizoroki-Heck, Suzuki-Miyaura, and Sonogashira reactions).<sup>93–98</sup> Other groups of oxyamine, hydrazide, and cyanobenzothiazole (Table 2) may also be used for the development of diazonium reagents for catalysis-free biolabeling.<sup>99,100</sup> In addition, some photo-induced reactive groups (*e.g.* 9,10-phenanthrenequinone and tetrazole)<sup>101–104</sup> should be possible for the preparation of new bench-stable diazonium reagents.

We also believe that different types of linkers (*e.g.* flexible PEG or rigid polyphenylene vinylene) could be introduced between the two diazonium cations to obtain new crosslinking reagents (Fig. 11a). Furthermore, new crosslinking reagents with three, four, and five diazonium tags (Fig. 11b) can be

**Table 2** Selected bioorthogonal reactions for the future development of bench-stable diazonium reagents

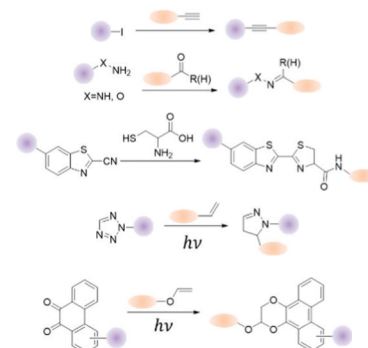
Palladium-mediated ligation

Oxime/hydrazone ligation

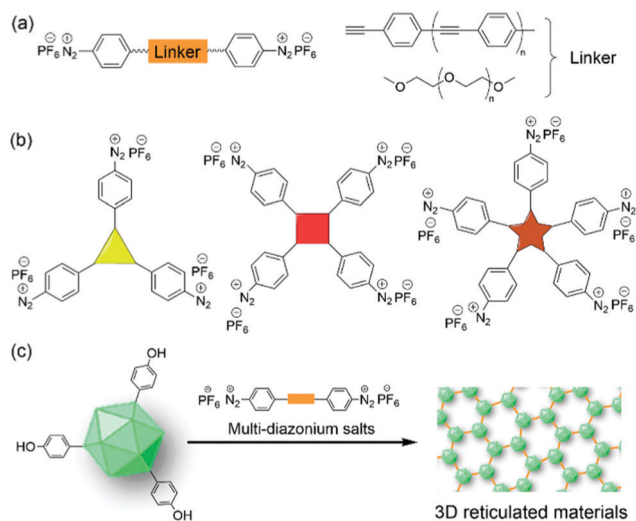
Cysteine-based ligation

Photo-induced 1,3-dipolar cycloadditions

Visible light-initiated photoclick cycloaddition







**Fig. 11** (a) Construction of new dual-diazonium reagents from different kinds of linkers (rigid or flexible structures). (b) Schematic illustration of triple-diazonium, quadruple-diazonium and quintuple-diazonium reagents. (c) Crosslinking of spherical viruses and multi-diazonium salts to generate 3D reticulated materials.

developed for the multiple cross-linking of biomolecules and viruses. Therefore, the development of bench-stable diazonium reagents is still in its infancy, and we hope that this review will facilitate the development of future reagents for biolabeling.

On the other hand, the size, length, and diameter of native TMV can be tuned in a controllable fashion by the combination of molecular biology and chemical biology methods. Therefore, there should be extremely large space for the construction of these TMV-based VLPs as nanotemplates for (in)organics as well as scaffolds for biotechnology. Additionally, the labeling of other plant virus nanostructures *via* the diazonium reagents will provide large chemical space for further modification and functionalization. For example, the preparation and properties of other biopolymer materials based on the combination of multi-diazonium reagents and other plant viruses can be further explored to provide novel 3D reticulated materials (Fig. 11c). Moreover, the plant virus-based hydrogels could be extended for biomedical and agriculture applications, including packing and releasing the antitumor drugs, defending plants from pathogenic attack, and so on. All in all, we hope that this minireview will facilitate the further development of multiple diazonium salts and their labeling with proteins/viruses for the preparation of new biomaterials including hydrogels.

## Conflicts of interest

The authors declare no competing financial interests.

## Acknowledgements

We thank Prof. Zhen Xi at Nankai University for kind support. This work was supported by NSFC (21572019, 21877008 and 22177010).

## Notes and references

- 1 C. Zhang, B. Wu, Y. Zhou, F. Zhou, W. Liu and Z. Wang, Mussel-inspired hydrogels: from design principles to promising applications, *Chem. Soc. Rev.*, 2020, **49**, 3605–3637.
- 2 E. M. Ahmed, Hydrogel: preparation, characterization, and applications: a review, *J. Adv. Res.*, 2015, **6**, 105–121.
- 3 W. F. Lai and Z. D. He, Design and fabrication of hydrogel-based nanoparticulate systems for *in vivo* drug delivery, *J. Controlled Release*, 2016, **243**, 269–282.
- 4 B.-X. Wang, W. Xu, Z. Yang and Y. Wu, and F. Pi, An overview on recent progress of the hydrogels: from material resources, properties, to functional applications, *Macromol. Rapid Commun.*, 2022, 2100785.
- 5 S. Mantha, S. Pillai, P. Khayambashi, A. Upadhyay, Y. Zhang, O. Tao, H. M. Pham and S. D. Tran, Smart hydrogels in tissue engineering and regenerative medicine, *Materials*, 2019, **12**, 3323.
- 6 L. Yang, R. Peltier, M. Zhang, D. Song, H. Huang, G. Chen, Y. Chen, F. Zhou, Q. Hao, L. Bian, M. L. He, Z. Wang, Y. Hu and H. Sun, Desuccinylation-triggered peptide self-assembly: live cell imaging of SIRT5 activity and mitochondrial activity modulation, *J. Am. Chem. Soc.*, 2020, **142**, 18150–18159.
- 7 S. An, E. J. Jeon, J. Jeon and S.-W. Cho, A serotonin-modified hyaluronic acid hydrogel for multifunctional hemostatic adhesives inspired by a platelet coagulation mediator, *Mater. Horiz.*, 2019, **6**, 1169–1178.
- 8 S. Talebian, M. Mehrli, N. Taebnia, C. P. Pennisi, F. B. Kadumudi, J. Foroughi, M. Hasany, M. Nikkhah, M. Akbari, G. Orive and A. Dolatshahi-Pirouz, Self-healing hydrogels: the next paradigm shift in tissue engineering?, *Adv. Sci.*, 2019, **6**, 1801664.
- 9 W. Li, Z. Yan, J. Ren and X. Qu, Manipulating cell fate: dynamic control of cell behaviors on functional platforms, *Chem. Soc. Rev.*, 2018, **47**, 8639–8684.
- 10 S. Li, S. Dong, W. Xu, S. Tu, L. Yan, C. Zhao, J. Ding and X. Chen, Antibacterial hydrogels, *Adv. Sci.*, 2018, **5**, 1700527.
- 11 Z. Wang, Y. Cong and J. Fu, Stretchable and tough conductive hydrogels for flexible pressure and strain sensors, *J. Mater. Chem. B*, 2020, **8**, 3437–3459.
- 12 H. Du, W. Liu, M. Zhang, C. Si, X. Zhang and B. Li, Cellulose nanocrystals and cellulose nanofibrils based hydrogels for biomedical applications, *Carbohydr. Polym.*, 2019, **209**, 130–144.
- 13 J. Li, R. Xing, S. Bai and X. Yan, Recent advances of self-assembling peptide-based hydrogels for biomedical applications, *Soft Matter*, 2019, **15**, 1704–1715.
- 14 M. C. Catoira, L. Fusaro, D. Di Francesco, M. Ramella and F. Boccafroschi, Overview of natural hydrogels for regenerative medicine applications, *J. Mater. Sci.: Mater. Med.*, 2019, **30**, 115.
- 15 L. Li, J. M. Scheiger and P. A. Levkin, Design and applications of photoresponsive hydrogels, *Adv. Mater.*, 2019, **31**, 1807333.



- 16 S. Yigit, R. Sanyal and A. Sanyal, Fabrication and functionalization of hydrogels through “click” chemistry, *Chem. – Asian J.*, 2011, **6**, 2648–2659.
- 17 W. Hu, Z. Wang, Y. Xiao, S. Zhang and J. Wang, Advances in crosslinking strategies of biomedical hydrogels, *Biomater. Sci.*, 2019, **7**, 843–855.
- 18 A. C. Daly, L. Riley, T. Segura and J. A. Burdick, Hydrogel microparticles for biomedical applications, *Nat. Rev. Mater.*, 2020, **5**, 20–43.
- 19 H. He, W. Tan, J. Guo, M. Yi, A. N. Shy and B. Xu, Enzymatic noncovalent synthesis, *Chem. Rev.*, 2020, **120**, 9994–10078.
- 20 C. Jiang, H. Huang, X. Kang, L. Yang, Z. Xi, H. Sun, M. D. Pluth and L. Yi, NBD-based synthetic probes for sensing small molecules and proteins: design, sensing mechanisms and biological applications, *Chem. Soc. Rev.*, 2021, **50**, 7436–7495.
- 21 K. L. Shantha and D. R.-K. Harding, Synthesis and evaluation of sucrose-containing polymeric hydrogels for oral drug delivery, *J. Appl. Polym. Sci.*, 2002, **84**, 2597–2604.
- 22 D. A. Gyles, L. D. Castro, J. O.-C. Silva and R. M. Ribeiro-Costa, A review of the designs and prominent biomedical advances of natural and synthetic hydrogel formulations, *Eur. Polym. J.*, 2017, **88**, 373–392.
- 23 X. Xu, V. V. Jerca and R. Hoogenboom, Bioinspired double network hydrogels: from covalent double network hydrogels via hybrid double network hydrogels to physical double network hydrogels, *Mater. Horiz.*, 2021, **8**, 1173–1188.
- 24 D. Ma, J. Zhang, C. Zhang, Y. Men, H. Sun, L. Y. Li, L. Yi and Z. Xi, A highly efficient dual-diazonium reagent for protein crosslinking and construction of a virus-based gel, *Org. Biomol. Chem.*, 2018, **16**, 3353–3357.
- 25 C. Dickmeis, L. Kauth and U. Commandeur, From infection to healing: the use of plant viruses in bioactive hydrogels, *Wiley Interdiscip. Rev.: Nanomed. Nanobiotechnol.*, 2021, **13**, e1662.
- 26 A. M. Wen and N. F. Steinmetz, Design of virus-based nanomaterials for medicine, biotechnology, and energy, *Chem. Soc. Rev.*, 2016, **45**, 4074–4126.
- 27 E. M. Plummer and M. Manchester, Viral nanoparticles and virus-like particles: platforms for contemporary vaccine design, *Wiley Interdiscip. Rev.: Nanomed. Nanobiotechnol.*, 2011, **3**, 174–196.
- 28 I. Yildiz, S. Shukla and N. F. Steinmetz, Applications of viral nanoparticles in medicine, *Curr. Opin. Biotechnol.*, 2011, **22**, 901–908.
- 29 K. Z. Lee, V. B. Pussepitiyalage, Y.-H. Lee, L. S. Loesch-Fries, M. T. Harris, S. Hemmati and K. V. Solomon, Engineering tobacco mosaic virus and its virus-like-particles for synthesis of biotemplated nanomaterials, *Biotechnol. J.*, 2021, **16**, 2000311.
- 30 D. S. Peabody, A viral platform for chemical modification and multivalent display, *J. Nanobiotechnol.*, 2003, **1**, 1–8.
- 31 A. D. Brown, L. Naves, X. Wang, R. Ghodssi and J. N. Culver, Carboxylate-directed in vivo assembly of virus-like nanorods and tubes for the display of functional peptides and residues, *Biomacromolecules*, 2013, **14**, 3123–3129.
- 32 K. J. Koudelka, G. Destito, E. M. Plummer, S. A. Trauger, G. Siuzdak and M. Manchester, Endothelial targeting of cowpea mosaic virus (CPMV) via surface vimentin, *PLoS Pathog.*, 2009, **5**, e1000417.
- 33 V. Vignali, B. S. Miranda, I. Lodoso-Torrecilla, C. A.-J. van Nesselroy, B. J. Hoogenberg, S. Dantuma, F. Hollmann, J. W. de Vries, E. M. Warszawik, R. Fischer, U. Commandeur and P. van Rijn, Biocatalytically induced surface modification of the tobacco mosaic virus and the bacteriophage M13, *Chem. Commun.*, 2018, **55**, 51–54.
- 34 T. Douglas and M. Young, Host-guest encapsulation of materials by assembled virus protein cages, *Nature*, 1998, **393**, 152.
- 35 J. N. Culver, Tobacco mosaic virus assembly and disassembly: determinants in pathogenicity and resistance, *Annu. Rev. Phytopathol.*, 2002, **40**, 287–308.
- 36 M.-C. Daniel, I. B. Tsvetkova, Z. T. Quinkert, A. Murali, M. De, V. M. Rotello, C. C. Kao and B. Dragnea, Role of surface charge density in nanoparticle-templated assembly of bromovirus protein cages, *ACS Nano*, 2010, **4**, 3853–3860.
- 37 A. J. Love, V. Makarov, I. Yaminsky, N. O. Kalinina and M. E. Taliany, The use of tobacco mosaic virus and cowpea mosaic virus for the production of novel metal nanomaterials, *Virology*, 2014, **449**, 133–139.
- 38 D. J. Evans, The bionanoscience of plant viruses: templates and synthons for new materials, *J. Mater. Chem.*, 2008, **18**, 3746–3754.
- 39 K.-B. G. Scholthof, Tobacco mosaic virus: a model system for plant biology, *Annu. Rev. Phytopathol.*, 2004, **42**, 13–34.
- 40 A. Klug, The tobacco mosaic virus particle: structure and assembly, *Philos. Trans. R. Soc., B*, 1999, **354**, 531–535.
- 41 P. Liu, Y. Ning, Q. Zhou, G. Mao and Z. Niu, One-dimensional rod-like tobacco mosaic virus: self-assembly and applications, *Prog. Chem.*, 2015, **27**, 1425–1434.
- 42 M. Knez, M. Sumser, A. M. Bittner, C. Wege, H. Jeske, T. P. Martin and K. Kern, Spatially selective nucleation of metal clusters on the tobacco mosaic virus, *Adv. Funct. Mater.*, 2004, **14**, 116–124.
- 43 L. Wu, J. Zang, L. A. Lee, Z. Niu, G. C. Horvath, V. Braxton, A. C. Wibowo, M. A. Bruckman, S. Ghoshroy, H.-C. zur Loye, X. Li and Q. Wang, Electrospinning fabrication, structural and mechanical characterization of rod-like virus-based composite nanofibers, *J. Mater. Chem.*, 2011, **21**, 8550–8557.
- 44 T. L. Schlick, Z. Ding, E. W. Kovacs and M. B. Francis, Dual-surface modification of the tobacco mosaic virus, *J. Am. Chem. Soc.*, 2005, **127**, 3718–3723.
- 45 M. A. Bruckman and N. F. Steinmetz, Chemical modification of the inner and outer surfaces of tobacco mosaic virus (TMV), *Methods Mol. Biol.*, 2014, **1108**, 173–185.
- 46 M. W. Jones, G. Mantovani, C. A. Blindauer, S. M. Ryan, X. Wang, D. J. Brayden and D. M. Haddleton, Direct peptide bioconjugation/PEGylation at tyrosine with linear and branched polymeric diazonium salts, *J. Am. Chem. Soc.*, 2012, **134**, 7406–7413.



- 47 S. Chen and M.-L. Tsao, Genetic incorporation of a 2-naphthol group into proteins for site-specific azo coupling, *Bioconjugate Chem.*, 2013, **24**, 1645–1649.
- 48 E. Royston, A. Ghosh, P. Kofinas, M. T. Harris and J. N. Culver, Self-assembly of virus-structured high surface area nanomaterials and their application as battery electrodes, *Langmuir*, 2008, **24**, 906–912.
- 49 H. Yi, S. Nisar, S.-Y. Lee, M. A. Powers, W. E. Bentley, G. F. Payne, R. Ghodssi, G. W. Rubloff, M. T. Harris and J. N. Culver, Patterned assembly of genetically modified viral nanotemplates via nucleic acid hybridization, *Nano Lett.*, 2005, **5**, 1931–1936.
- 50 U. Gallwize, L. King and R. N. Perham, Preparation of an isomorphous heavy-atom derivative of tobacco mosaic virus by chemical modification with 4-sulpho-phenylisothiocyanate, *J. Mol. Biol.*, 1974, **87**, 257–260.
- 51 M. L. Smith, J. A. Lindbo, S. Dillard-Telm, P. M. Brosio, A. B. Lasnik, A. A. McCormick, L. V. Nguyen and K. E. Palmer, Modified tobacco mosaic virus particles as scaffolds for display of protein antigens for vaccine applications, *Virology*, 2006, **348**, 475–488.
- 52 L. A. Lee, H. G. Nguyen and Q. Wang, Altering the landscape of viruses and bionanoparticles, *Org. Biomol. Chem.*, 2011, **9**, 6189–6195.
- 53 R. A. Miller, A. D. Presley and M. B. Francis, Self-assembling light-harvesting systems from synthetically modified tobacco mosaic virus coat proteins, *J. Am. Chem. Soc.*, 2007, **129**, 3104–3109.
- 54 X. Liu, B. Liu, S. Gao, Z. Wang, Y. Tian, M. Wu, S. Jiang and Z. Niu, Glyco-decorated tobacco mosaic virus as a vector for cisplatin delivery, *J. Mater. Chem. B*, 2017, **5**, 2078–2085.
- 55 D. L. Kernan, A. M. Wen, A. S. Pitek and N. F. Steinmetz, Delivery of chemotherapeutic vcMMAE using tobacco mosaic virus nanoparticles, *Exp. Biol. Med.*, 2017, **242**, 1405–1411.
- 56 O. Jacobson, D. O. Kiesewetter and X. Chen, Interface of physics and biology: engineering virus-based nanoparticles for biophotonics, *Bioconjugate Chem.*, 2015, **26**, 51–62.
- 57 Z. Yin, H. G. Nguyen, S. Chowdhury, P. Bentley, M. A. Bruckman, A. Miermont, J. C. Gildersleeve, Q. Wang and X. Huang, Tobacco mosaic virus as a new carrier for tumor associated carbohydrate antigens, *Bioconjugate Chem.*, 2012, **23**, 1694–1703.
- 58 Y. Tian, S. Gao, M. Wu, X. Liu, J. Qiao, Q. Zhou, S. Jiang and Z. Niu, Tobacco mosaic virus-based 1D nanorod-drug carrier via the integrin-mediated endocytosis pathway, *ACS Appl. Mater. Interfaces*, 2016, **8**, 10800–10807.
- 59 A. E. Czapar, Y.-R. Zheng, I. A. Riddell, S. Shukla, S. G. Awuah, S. J. Lippard and N. F. Steinmetz, Tobacco mosaic virus delivery of phenanthriplatin for cancer therapy, *ACS Nano*, 2016, **10**, 4119–4126.
- 60 S. Chu, A. D. Brown, J. N. Culver and R. Ghodssi, Tobacco mosaic virus as a versatile platform for molecular assembly and device fabrication, *Biotechnol. J.*, 2018, **13**, 1800147.
- 61 X. Z. Fan, E. Pomerantseva, M. Gnerlich, A. Brown, K. Gerasopoulos, M. McCarthy, J. Culver and R. Ghodssi, Tobacco mosaic virus: a biological building block for micro/nano/bio systems, *J. Vac. Sci. Technol., A*, 2013, **31**, 050815.
- 62 C. Koch, F. J. Eber, C. Azucena, A. Förste, S. Walheim, T. Schimmel, A. M. Bittner, H. Jeske, H. Gliemann, S. Eiben, F. C. Geiger and C. Wege, Novel roles for well-known players: from tobacco mosaic virus pests to enzymatically active assemblies, *Beilstein J. Nanotechnol.*, 2016, **7**, 613–629.
- 63 C. Hou, H. Xu, X. Jiang, Y. Li, S. Deng, M. Zang, J. Xu and J. Liu, Virus-based supramolecular structure and materials: concept and prospects, *ACS Appl. Bio Mater.*, 2021, **4**, 5961–5974.
- 64 M. A. Bruckman, S. Hern, K. Jiang, C. A. Flask, X. Yu and N. F. Steinmetz, Tobacco mosaic virus rods and spheres as supramolecular high-relaxivity MRI contrast agents, *J. Mater. Chem. B*, 2013, **1**, 1482–1490.
- 65 D. Ma, Y. Xie, J. Zhang, D. Ouyang, L. Yi and Z. Xi, Self-assembled controllable virus-like nanorods as templates for construction of one-dimensional organic–inorganic nanocomposites, *Chem. Commun.*, 2014, **50**, 15581–15584.
- 66 Z. Niu, M. Bruckman, V. S. Kotakadi, J. He, T. Emrick, T. P. Russell, L. Yang and Q. Wang, Study and characterization of tobacco mosaic virus head-to-tail assembly assisted by aniline polymerization, *Chem. Commun.*, 2006, 3019–3021.
- 67 J. M. Rego, J.-H. Lee, D. H. Lee and H. Yi, Biologically inspired strategy for programmed assembly of viral building blocks with controlled dimensions, *Biotechnol. J.*, 2013, **8**, 237–246.
- 68 C. P. Ramil and Q. Lin, Bioorthogonal chemistry: strategies and recent developments, *Chem. Commun.*, 2013, **49**, 11007–11022.
- 69 C. S. McKay and M. G. Finn, Click chemistry in complex mixtures: bioorthogonal bioconjugation, *Chem. Biol.*, 2014, **21**, 1075–1101.
- 70 O. Boutureira and G. J.-L. Bernardes, Advances in chemical protein modification, *Chem. Rev.*, 2015, **115**, 2174–2195.
- 71 J. Li and P. R. Chen, Development and application of bond cleavage reactions in bioorthogonal chemistry, *Nat. Chem. Biol.*, 2016, **12**, 129–137.
- 72 B. L. Oliveira, Z. Guo and G. J.-L. Bernardes, Inverse electron demand Diels–Alder reactions in chemical biology, *Chem. Soc. Rev.*, 2017, **46**, 4895–4950.
- 73 T. K. Heiss, R. S. Dorn and J. A. Prescher, Bioorthogonal reactions of triarylphosphines and related analogues, *Chem. Rev.*, 2021, **121**, 6802–6849.
- 74 F.-G. Zhang, Z. Chen, X. Tang and J.-A. Ma, Triazines: syntheses and inverse electron-demand Diels–Alder reactions, *Chem. Rev.*, 2021, **121**, 14555–14593.
- 75 V. M. Lechner, M. Nappi, P. J. Deneny, S. Folliet, J. C.-K. Chu and M. J. Gaunt, Visible-light-mediated modification and manipulation of biomacromolecules, *Chem. Rev.*, 2022, **122**, 1752–1829.
- 76 V. V. Rostovtsev, L. G. Green, V. V. Fokin and K. B. Sharpless, A stepwise Huisgen cycloaddition process: copper(I)-catalyzed regioselective “ligation” of azides and terminal alkynes, *Angew. Chem., Int. Ed.*, 2002, **41**, 2596–2599.





- 77 M. A. Bruckman, G. Kaur, L. A. Lee, F. Xie, J. Sepulveda, R. Breitenkamp, X. Zhang, M. Joralemon, T. P. Russell, T. Emrick and Q. Wang, Surface modification of tobacco mosaic virus with “click” chemistry, *ChemBioChem*, 2008, **9**, 519–523.
- 78 X. Zhao, L. Chen, J. A. Luckanagul, X. Zhang, Y. Lin and Q. Wang, Enhancing antibody response against small molecular hapten with tobacco mosaic virus as a polyvalent carrier, *ChemBioChem*, 2015, **16**, 1279–1283.
- 79 P. Sitasuwan, L. A. Lee, K. Li, H. G. Nguyen and Q. Wang, RGD-conjugated rod-like viral nanoparticles on 2D scaffold improve bone differentiation of mesenchymal stem cells, *Front. Chem.*, 2014, **2**, 31.
- 80 V. Vignali, B. S. Miranda, I. Lodoso-Torrecilla, C. A.-J. van Nesselroy, B.-J. Hoogenberg, S. Dantuma, F. Hollmann, J. W. de Vries, E. M. Warsawik, R. Fischer, U. Commandeure and P. van Rijn, Biocatalytically induced surface modification of the tobacco mosaic virus and the bacteriophage M13, *Chem. Commun.*, 2019, **55**, 51–54.
- 81 J. Gavriluk, H. Ban, M. Nagano, W. Hakamata and C. F. Barbas III, Formylbenzene diazonium hexafluorophosphate reagent for tyrosine-selective modification of proteins and the introduction of a bioorthogonal aldehyde, *Bioconjugate Chem.*, 2012, **23**, 2321–2328.
- 82 L. Lv, *The size control of tobacco mosaic virus nanoparticle and the modification of its coat protein*, Master thesis, Nankai University, China, 2012.
- 83 J. Zhang, D. Ma, D. Du, Z. Xi and L. Yi, An efficient reagent for covalent introduction of alkynes into proteins, *Org. Biomol. Chem.*, 2014, **12**, 9528–9531.
- 84 R. J. Blizzard, D. R. Backus, W. Brown, C. G. Bazewicz, Y. Li and R. A. Mehl, Ideal bioorthogonal reactions using a site-specifically encoded tetrazine amino acid, *J. Am. Chem. Soc.*, 2015, **137**, 10044.
- 85 J. Wang, X. Wang, X. Fan and P. R. Chen, Unleashing the power of bond cleavage chemistry in living systems, *ACS Cent. Sci.*, 2021, **7**, 929–943.
- 86 J. Zhang, Y. Men, S. Lv, L. Yi and J. F. Chen, Protein tetrazinylation via diazonium coupling for covalent and catalyst-free bioconjugation, *Org. Biomol. Chem.*, 2015, **13**, 11422–11425.
- 87 J. Zhang, Y. Gao, X. Kang, Z. Zhu, Z. Wang, Z. Xi and L. Yi, o,o-Difluorination of aromatic azide yields a fast-response fluorescent probe for H<sub>2</sub>S detection and for improved bioorthogonal reactions, *Org. Biomol. Chem.*, 2017, **15**, 4212–4217.
- 88 Y. Xie, L. Cheng, Y. Gao, X. Cai, X. Yang, L. Yi and Z. Xi, Tetrafluorination of aromatic azide yields a highly efficient Staudinger reaction: kinetics and biolabeling, *Chem. – Asian J.*, 2018, **13**, 1791–1796.
- 89 M. Sundhoro, S. Jeon, J. Park, O. Ramström and M. Yan, Perfluoroaryl azide Staudinger reaction: a fast and bioorthogonal reaction, *Angew. Chem., Int. Ed.*, 2017, **56**, 12117–12121.
- 90 D. Ma, X. Kang, Y. Gao, J. Zhu, L. Yi and Z. Xi, Design and synthesis of a highly efficient labelling reagent for incorporation of tetrafluorinated aromatic azide into proteins, *Tetrahedron*, 2019, **75**, 888–893.
- 91 D. Ma, Z. Chen, L. Yi and Z. Xi, Development of improved dual-diazonium reagents for faster crosslinking of tobacco mosaic virus to form hydrogels, *RSC Adv.*, 2019, **9**, 29070–29077.
- 92 M. Hridoy, M. Z.-H. Gorapi, S. Noor, N. S. Chowdhury, M. M. Rahman, I. Muscari, F. Masia, S. Adorisio, D. V. Delfino and M. A. Mazid, Putative anticancer compounds from plant-derived endophytic fungi: a review, *Molecules*, 2022, **27**, 296.
- 93 M. Yang, J. Li and P. R. Chen, Transition metal-mediated bioorthogonal protein chemistry in living cells, *Chem. Soc. Rev.*, 2014, **43**, 6511–6526.
- 94 K. Kodama, S. Fukuzawa, H. Nakayama, K. Sakamoto, T. Kigawa, T. Yabuki, N. Matsuda, M. Shirouzu, K. Takio, S. Yokoyama and K. Tachibana, Site-specific functionalization of proteins by organopalladium reactions, *ChemBioChem*, 2007, **8**, 232–238.
- 95 N. Li, R. K.-V. Lim, S. Edwardraja and Q. Lin, Copper-free Sonogashira cross-coupling for functionalization of alkyne-encoded proteins in aqueous medium and in bacterial cells, *J. Am. Chem. Soc.*, 2011, **133**, 15316–15319.
- 96 J. Li, S. Lin, J. Wang, S. Jia, M. Yang, Z. Hao, X. Zhang and P. R. Chen, Ligand-free palladium-mediated site-specific protein labeling inside Gram-negative bacterial pathogens, *J. Am. Chem. Soc.*, 2013, **135**, 7330–7338.
- 97 S. V. Chankeshwara, E. Indrigo and M. Bradley, Palladium-mediated chemistry in living cells, *Curr. Opin. Chem. Biol.*, 2014, **21**, 128–135.
- 98 J. M. Chalker, C. S.-C. Wood and B. G. Davis, A convenient catalyst for aqueous and protein Suzuki-Miyaura cross-coupling, *J. Am. Chem. Soc.*, 2009, **131**, 16346–16347.
- 99 H. F. Gaertner, K. Rose, R. Cotton, D. Timms, R. Camble and R. E. Offord, Construction of protein analogues by site-specific condensation of unprotected fragments, *Bioconjugate Chem.*, 1992, **3**, 262–268.
- 100 H. Ren, F. Xiao, K. Zhan, Y.-P. Kim, H. Xie, Z. Xia and J. Rao, A biocompatible condensation reaction for the labeling of terminal cysteine residues on proteins, *Angew. Chem., Int. Ed.*, 2009, **48**, 9658–9662.
- 101 J. Li, H. Kong, L. Huang, B. Cheng, K. Qin, M. Zheng, Z. Yan and Y. Zhang, Visible light-initiated bioorthogonal photoclick cycloaddition, *J. Am. Chem. Soc.*, 2018, **140**, 14542–14546.
- 102 H. Huang, G. Zhang, L. Gong, S. Zhang and Y. Chen, Visible-light-induced chemoselective deboronative alkynylation under biomolecule-compatible conditions, *J. Am. Chem. Soc.*, 2014, **136**, 2280–2283.
- 103 Y. Wang, W. J. Hu, W. Song, R. K.-V. Lim and Q. Lin, Discovery of long-wavelength photoactivatable diaryltetrazoles for bioorthogonal 1,3-dipolar cycloaddition reactions, *Org. Lett.*, 2008, **10**, 3725–3728.
- 104 W. Song, Y. Wang, J. Qu, M. M. Madden and Q. Lin, A photoinducible 1,3-dipolar cycloaddition reaction for rapid, selective modification of tetrazole-containing proteins, *Angew. Chem., Int. Ed.*, 2008, **47**, 2832–2835.
- 105 T. Deb, J. Tu and R. M. Franzini, Mechanisms and substituent effects of metal-free bioorthogonal reactions, *Chem. Rev.*, 2021, **121**, 6850–6914.

